

# Optical Ranging: Asynchronous-Mode Concept, Prototype and Validation

Marc Sanchez Net\*

ABSTRACT. — This article describes an asynchronous system to estimate the range between a spacecraft and a ground station from an optical or RF uplink, and an optical downlink. It is built as an improvement over Optical Telemetry Ranging, a method described in a previous article, which adapted the basic principles of RF Telemetry Ranging to optical links and standards.

The fundamental principle of an asynchronous ranging system is that range measurements should be recovered without needing to synchronize the uplink receiver and the downlink transmitter on board the spacecraft (hence the name asynchronous). To do so, the observables required for the range computation are obtained at the ground station's uplink subsystem and at the spacecraft's uplink receiver, instead of the ground station's uplink and downlink subsystems. The measurement obtained on board the spacecraft is then sent back to Earth, as part of telemetry, where it is time-tagged and post-processed for range recovery purposes.

The article is divided into two parts. First, it provides an overview of an asynchronous ranging system with specific emphasis on the proposed modifications to the previous Optical Telemetry Ranging. Then, it describes a software prototype developed at the Jet Propulsion Laboratory to validate its operation under representative channel conditions expected for the Deep Space Optical Communications terminal on board the Psyche spacecraft.

---

\*Communications Architectures and Research Section.

The research described in this publication was carried out by the Jet Propulsion Laboratory, California Institute of Technology, under a contract with the National Aeronautics and Space Administration. © 2023. California Institute of Technology. Government sponsorship acknowledged.

## I. Introduction

A previous article described an synchronous ranging system<sup>1</sup> that operates with an optical uplink and downlink and can be used to determine the distance between a spacecraft and a ground station [1]. Similarly, another article described the concept behind Optical Telemetry Ranging [2], an adaptation of RF Telemetry Ranging [3, 4] for the case where the uplink and/or the downlink operate in the optical domain. In the present article, we describe updates to the proposed method that simplify its implementation when used in conjunction with the Consultative Committee for Space Data Systems (CCSDS) High Photon Efficiency (HPE) standard [5, 6]. We also show how the proposed system can be used in a hybrid architecture in which the uplink uses traditional CCSDS-compliant RF signaling schemes, while the downlink uses HPE signaling.

The second part of this article is devoted to describing a software prototype built at the Jet Propulsion Laboratory (JPL) to validate the system operation. In that sense, we first describe the basic structure of the prototype and then demonstrate its performance under representative channel conditions, which we obtain from trajectories and specifications from the Deep Space Optical Communications (DSOC) terminal on board the Psyche spacecraft.

## II. Asynchronous Ranging System

This section describes the basic principle of operation for an asynchronous ranging system. It expands concepts introduced in a previous article [2], and leverages the ranging formulation described in References [3, 4]. Hence, the reader is pointed to those articles for further details and clarifications on the methods, techniques, and the related mathematical notation.

### A. The Ranging Codeword

Consider a spacecraft communicating with a ground station via a simultaneous uplink and downlink. Assume that data is being transferred bidirectionally, encoded using CCSDS transfer frames that are then encapsulated as a stream of possibly interleaved data-carrying codewords, separated using synchronization markers known to both the transmitter and receiver. Then, we define a *ranging codeword* (RCW) as a sequence of  $N$  consecutive synchronization-marked codewords (SMCW), where each SMCW starts with a synchronization marker and it is followed by one or multiple data codewords

---

<sup>1</sup>The principle of operation of a synchronous ranging system is akin to a regenerative ranging system in the RF domain because the downlink transmit clock is “regenerated” from the received uplink clock. In an asynchronous system, we eliminate the need to “regenerate” the downlink clock by making a phase measurement directly on the received uplink signal. As explained later, this measurement does not have a time-tag associated with it, so the spacecraft requires a “good enough” time and frequency reference for the phase measurement only.

and, possibly, a tail sequence (see Figure 1). The number  $N$  is chosen to ensure the ranging system has enough ambiguity resolution and may be different on the uplink and downlink channels. Also, for the system to operate correctly, the value  $N$  is known a priori by both the transmitter and receiver.

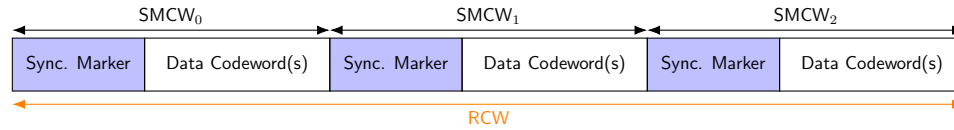


**Figure 1. Structure of a RCW assuming it contains  $N = 3$  SMCWs. Tail sequences are not shown for the sake of clarity, but they might be present if the format of the SMCW requires it.**

Each RCW is identified by a *ranging codeword identifier* (RCID), which is defined as the first  $S$  symbols following the end of the first synchronization marker in the RCW, and is designed such that the probability of having multiple RCWs with the same RCID is low. Several noteworthy remarks follow:

- In practice, the choice of  $S$  will depend on the characteristics of the data link layer (e.g., transfer frame format, encoding, interleaving, etc.). For example, in systems without interleavers, it may be advantageous to select  $S$  such that the header of the CCSDS transfer frame is included in the RCID. This header contains a counter that increases with every transfer frame, thus ensuring the RCID is unique.
- Because the uplink and downlink might have different signaling formats, the length and format of the uplink and downlink RCIDs might also be different.
- Unlike synchronization markers, RCIDs are not designed to have good autocorrelation properties. Therefore, in a noisy environment, RCIDs are better measured after decoding the received data stream, instead of using symbols obtained via hard-decision at the demodulator output.
- RCID are used to associate timestamps measured at the ground station with phase measurements on board the spacecraft. Hence, their main purpose is to identify an RCW within a sequence of RCWs. In practice, this means that even if two or more RCWs have the same RCID, this association process is still possible by performing a cross-correlation operation over two sequences of RCIDs, one received from the spacecraft and another measured in the ground station downlink subsystem.
- In Optical Telemetry Ranging [2], transfer frames were used in lieu of ranging codewords, and frame identifiers (i.e., transfer frame primary headers) were used instead of RCIDs. These original definitions were inherited from RF Telemetry Ranging but have been abandoned in this article due to the presence of an interleaver in the HPE standard. This interleaver makes it difficult to recover the frame identifier in real time, since its symbols might be spread across

multiple codewords. Hence, we propose here a new definition of RCW and RCID that applies directly to the stream of symbols transferred over the channel (i.e., interleaved symbols, if an interleaver is used), thus simplifying the operation and implementation of the ranging system.

### B. Phase of a Ranging Codeword

The phase of the uplink and/or downlink signals is defined as the possibly fractional number of symbols that have elapsed since the start of the RCW (i.e., the start of the first synchronization marker) [1, 2]. Here, exact meaning of “symbol” is arbitrary and depends on the signaling format over the link. For example, in an RF link, a symbol could be a 0 or 1 (in unipolar convention) coming out of the encoder prior to modulation. In contrast, in HPE telemetry a “symbol” could be a slot, if the phase is measured in slots, or a PPM symbol, if by convention PPM symbols are used instead. In fact, all that matters is that there is consistency in the definition of a “symbol” within the ranging system or that constant conversion factors are properly applied if uplink and downlink phases are measured using different units.<sup>2</sup>

Phases can be measured in a wrapped or unwrapped form. In the former approach, the wrapped phase ranges from 0 to a maximum value  $P$  that depends on the length of the RCW and starts again at 0 with every new RCW. This makes it ideal for recording the phase in a finite number of bits, as would be the case when transmitting it from the spacecraft to Earth. Alternatively, unwrapped phases start at 0 at the beginning of the first RCW, which is selected arbitrarily, and take values  $iP$ ,  $i \geq 1$  at the start of all subsequent ranging codewords in the data stream. This structure is shown in Figure 2, which uses the symbols  $\psi$  and  $\tilde{\psi}$  to denote unwrapped and wrapped phases, respectively, a convention used henceforth.

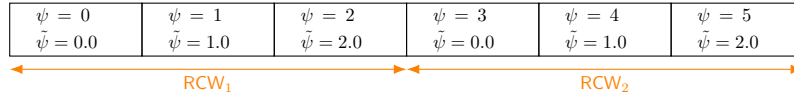


**Figure 2. Example of a wrapped and unwrapped phase in a RCW with  $P = 3$ . Each square represents one symbol.**

Finally, the HPE standard defines the concept of repeated symbols for the purpose of increasing the total received power to and enabling operation at low signal conditions. We argue that such repeated symbols should not be used for the purpose of defining the phase, nor should they be used to count the number  $S$  of symbols forming an RCID. Similarly, the definition of the RCW phase should not depend in any way on the modulation format used to transmit the information, be it in the RF or the optical domain.

---

<sup>2</sup>An example of such conversion is reported in [1], where a factor  $\beta$  is applied in the ranging equation (Equation 33 in [1]) to capture the fact that the downlink phase is measured in units of downlink PPM slots, while the uplink phase is measured in uplink PPM symbols.

### C. Concept of Operations

We now describe the concept of operations of the asynchronous ranging system, which is divided in three parts:

1. Collect and time-tag phase measurements at the ground station and on board the spacecraft. These measurements are known as ranging observables.
2. Recover an estimate of the round-trip light-time (RTLTL) by processing the ranging observables, either in real-time during the ranging track, or later in post-processing.
3. Estimate the distance to the spacecraft from RTLTL measurements, prior spacecraft state information, and other externally known data (e.g., gravity field models).

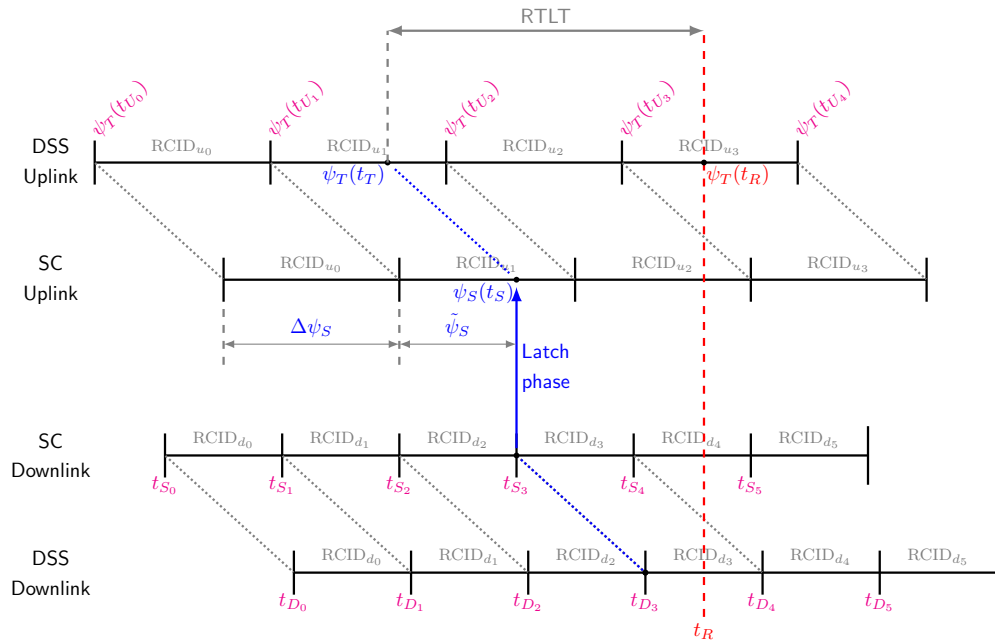


**Figure 3. Concept of Operations for the Asynchronous Ranging System.**

We now explain how the ranging system operates for each of these steps.<sup>3</sup> In that sense, Figure 3 graphically depicts the set of phase measurements collected by the system and the instants in time when they are collected. In particular, we show that:

- 1.1 The ground station's uplink subsystem records the time of departure of each RCW in the uplink, its associated RCID, and the phase of the uplink signal

<sup>3</sup>Except for steps (1.2) and (1.3), all functions are assumed to be performed at the Earth station.

which is just a monotonically increasing counter. These values form a sequence of tuples, one per departing RCW, which we denote  $\{t_U, \psi_T, \text{RCID}_u\}$ .<sup>4</sup>

- 1.2 During the ranging track, the spacecraft receiver records ranging observables every time a downlink RCW departs (or a constant time after), an event we denote by  $t_S$ . Each ranging observable contains three quantities: The wrapped phase of the received uplink RCW, its RCID, and the RCID of the RCW that triggered the measurement. Let  $\{\tilde{\psi}_S, \text{RCID}_u, \text{RCID}_d\}$  denote this set of collected ranging observables, noting that  $t_S$  is not recorded because we do not presume that the spacecraft has a good enough clock to perform such a measurement. Also, at the beginning of the ranging track, the spacecraft is free to choose which uplink SMCW is the start of the first uplink RCW and which downlink SMCW is the start of the first downlink RCW.
- 1.3 The spacecraft places the phases measured in step (1.2) in the downlink telemetry stream, which may or may not be sent concurrently with the tracking session. For example, an implementation may choose to record the phase measurements during a ranging track and send them to Earth in a subsequent track, hours later.
- 1.4 During the ranging track, the ground station's downlink subsystem measures the time of arrival of each RCW and its associated RCID, effectively gathering a set of observables that we denote by  $\{t_D, \text{RCID}_d\}$ .

Next, we describe how an estimate of the round-trip light-time (RTLTL) delay between the spacecraft and the ground station can be obtained from the previous measurements (step 2). This process may be performed in near-real time, during the ranging track, or it may be performed in post-processing, using the information recorded at the ground station. Either way, assume the system wishes to calculate the two-way propagation delay at a set of discrete instants of time  $\{t_R\}$  which, for simplicity, we assume equal to  $\{t_D\}$ .<sup>5</sup> The RTLTL recovery mechanism works as follows:

- 2.1 At each  $t_R$ , the system estimates the phase of the station's uplink subsystem  $\psi_T$  and its associated  $\text{RCID}_u$ . This can be done via interpolation over  $\{t_U, \psi_T\}$  obtained in step (1.1) because, by construction,  $\min\{t_U\} < t_R < \max\{t_U\}$ .
- 2.2 At each  $t_R$ , the system estimates the RCID of the downlink RCW arriving at that point in time using the measurements  $\{t_D, \text{RCID}_d\}$  from step (1.4). Let

---

<sup>4</sup>We use  $\{a, b, c\}$  to denote a set of tuples, i.e.,  $\{a, b, c\} = \{(a_1, b_1, c_1), (a_2, b_2, c_2), \dots\}$ , where the sub-index in each tuple is used to indicate measurements at monotonically increasing instants of time. Similarly, the set formed by each element of the tuples is denoted by  $\{a\} = \{a_1, a_2, \dots\}$ ,  $\{b\} = \{b_1, b_2, \dots\}$ , etc. Finally, we use  $a, b$ , etc., to denote a value within the set  $\{a\}$ ,  $\{b\}$ , etc., for the sake of simplicity in our notation.

<sup>5</sup>Figure 3 shows  $t_D$  and  $t_R$  as different. Indeed, in a real operational system, these instants of time need not be the same because the range recovery mechanism may estimate the RTLTL at any arbitrary  $t_R$  using interpolation.

$\{t_R, \text{RCID}_d\}$  denote the output of this operation.

- 2.3 The system uses each  $\text{RCID}_d$  from step (2.2) to associate  $t_R$  with a measurement on board the spacecraft obtained in step (1.2). This is possible because all spacecraft measurements contain the  $\text{RCID}_d$  of the RCW that triggered the phase measurement, so their values can be compared directly with  $\text{RCID}_d$ s recorded on the ground. The output of this operation is  $\{t_R, \tilde{\psi}_S, \text{RCID}_u\}$ .
- 2.4 The output of step (2.3) contains a phase estimate  $\tilde{\psi}_S$  that is wrapped. However, for the range computation, we need to operate over unwrapped phases, i.e., we need to recover  $\psi_S$ . To do so, the system compares the uplink RCID obtained from steps (1.1) and (1.3) and calculates the absolute phase offset  $\Delta\psi_S$  of each RCW. This is akin to finding the relative position of a given RCW in the sequence of RCWs transmitted over the uplink.
- 2.5 The system calculates the unwrapped phase as  $\psi_S = \Delta\psi_S + \tilde{\psi}_S$ . The output of this operation is a sequence of measurements  $\{t_R, \psi_S\}$ .
- 2.6 The system calculates the derivative of the transmit phase, denoted  $\dot{\psi}_T$ , using  $\{t_U, \psi_T\}$  from step (1.1). In cases where the station's uplink subsystem is not applying range-rate pre-compensation, this value is constant. Otherwise, numerical differentiation is used.
- 2.7 The system calculates the two-way propagation delay by solving Equation (1), the fundamental ranging equation for an asynchronous ranging system.<sup>6</sup> Note that this is the discrete version of the equation reported in [3]. Note also that in (1) the only unknown is  $t_T$  and that, once solved numerically, the two-way propagation delay is simply  $\tau = t_R - t_T$ .

$$\sum_{t_T}^{t_R} \dot{\psi}_T = \psi_T - \psi_S \quad (1)$$

Once the system has obtained an estimate of the two-way propagation delay  $\tau$ , then a range estimate  $d$  can also be obtained by relating these two quantities (step 3). In general, this step is non-trivial and must consider changes in the speed of light due to the atmosphere; prior knowledge about the spacecraft motion, including estimates of the spacecraft trajectory and relative range rate; gravity field models, if available; and aberration and relativistic corrections, among others. For example in [1] we show the expressions relating propagation delay and distance for a linear trajectory with and without spacecraft measurement delays and assuming that the electromagnetic waves always travel at the speed of light. Even in this simplified scenario, the equations relating range and propagation delay are complex, and care must be exercised when associating a range estimate with its corresponding time.

---

<sup>6</sup>In Equation (1) we have implicitly assumed that all phases and their derivatives are expressed in the same units. If that is not the case, constant conversion factors must be applied.

## D. Operation with RF Uplinks

### 1. RF Uplink with Data

We first consider the case where the uplink operates in the RF domain and the downlink operates in the optical domain. In this case, it is assumed that the ground station transmits a sequence of Command Link Transmission Units (CLTUs) formatted according to [7], or a sequence of Channel Access Data Units (CADUs), formatted according to [8]. The symbols in these CLTUs or CADUs are phase modulated onto an RF carrier according to Reference [9], a process that is transparent to the asynchronous ranging system. Hence, operation of the system is possible regardless of the signaling scheme, a desirable feature in deep space operations since multiple modulation formats are typically used over a mission's lifetime.

Under these assumptions, the concept of operations as previously described remains unchanged, with uplink data being received via a traditional RF radio, while downlink data will be sent over an optical payload. The only accommodation necessary is that both the RF radio and the optical payload synchronize the time of departure of a downlink transmit frame with the latching instant at which a uplink phase  $\tilde{\psi}_S$  is measured.<sup>7</sup>

### 2. RF Uplink with a PN Sequence

The proposed asynchronous ranging system can also operate in the case that the RF uplink channel carries a PN sequence for ranging purposes [10], although some accommodations are needed in this case. In particular:

- The notion of an uplink ranging codeword does not exist. Instead, the PN sequence itself serves as the basis for calculating the phases  $\psi_T$  and  $\psi_S$ . In other words, the concept of operations as previously described remains valid, but  $\psi_T$  and  $\psi_S$  represent the possibly fractional number of PN chips elapsed since the beginning of the PN sequence.
- The RCID of the uplink is also undefined. However, range measurements can still be recovered because the PN sequence is long enough that no range ambiguity problems occur (or, more precisely, they can be resolved in the ground, in post-processing, using prior information on the spacecraft position). Therefore, the wrapped and unwrapped version of the measured uplink phase are equal.

---

<sup>7</sup>In reality the two events need not be perfectly synchronized. What really matters is that the latching instant occurs after a certain delay after the departure of a downlink transfer frame and that this delay is constant and known throughout a ranging track.



### III. Software Prototype

A software-based implementation of the described asynchronous ranging system has been implemented at JPL, using an architecture that is based on a previous implementation of a synchronous ranging system [1]. The simulator runs the uplink and downlink sequentially and lets the user select the signal format characteristics for both the uplink and downlink. For example, the tests shown later in this article will show how the prototype can be used using either a PN sequence, an RF signal, or HPE telemetry on the uplink, as well as HPE telemetry on the downlink.<sup>8</sup>

Figure 4 shows the high-level architecture of the prototype. As previously stated, the main interface between the uplink and downlink is the clock of the downlink RCWs (red arrow), which indicates the instants in time at which the spacecraft receive subsystem must measure the received uplink phase. In a real system implementation, there would be a second interface from the spacecraft receiver to the spacecraft transmitter (possibly indirectly through the flight computer) to deliver the collected phase measurements for inclusion in the spacecraft telemetry. However, our implementation obviates this step. Instead, the measurements are made available to the ground station downlink subsystem directly, which then processes them to extract the range estimate. There are two reasons that justify this simplification: First, the purpose of the prototype is to validate the asynchronous ranging system, not data transmission over an RF or optical link. Second, in a noisy channel, error-free recovery of the phase measurements arriving via telemetry can only be done after decoding the received data stream, which necessitates implementing multiple decoders, one per downlink format supported. This not only increases the required development effort, but it also increases the prototype's computational complexity and reduces its runtime performance.

The prototype is implemented in MATLAB, with part of its functionality compiled to C for faster execution. As with the synchronous mode, two modes of operation are possible, one intended for debugging purposes and another one for real system validation. In debug mode, the prototype assumes that the ground and spacecraft clocks are synchronized, and the entire simulation is run sequentially, storing the required information in random-access memory (RAM). Alternatively, in normal mode the simulator introduces a clock offset  $\Delta t$  between the ground station and spacecraft clock and can run iteratively, using state variables to store the necessary information between consecutive iterations. This can be used to perform significantly longer runs, thus helping us validate the system even if long receiver synchronization transients are present.

For optical links, a detailed description of the different elements in Figure 4 and their implementation can be found in Reference [1]. For RF links, the prototype currently

---

<sup>8</sup>The prototype is currently being upgraded so that it can also operate using HPE Beacon plus accompanying data [6] on the uplink.

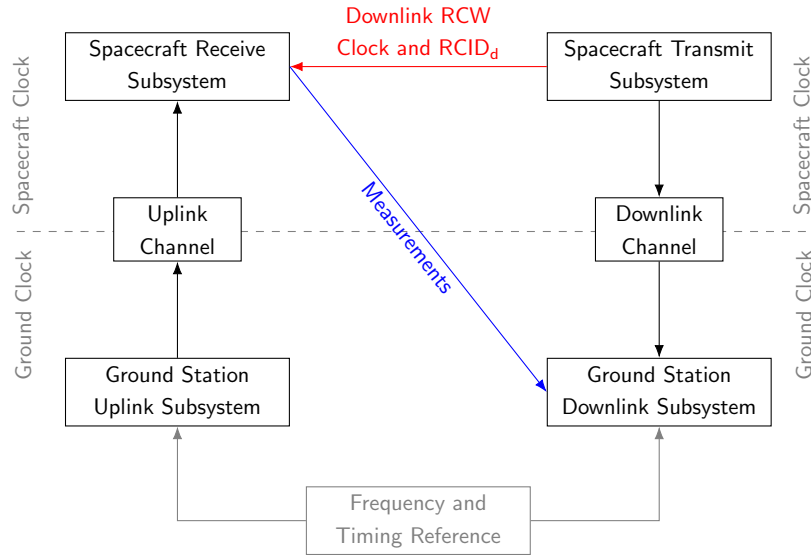


**Figure 4. High-Level Functionality for an Asynchronous Ranging System. Modified from [1].**

operates in the complex baseband domain and assumes that the signal (either data or a PN sequence) is phase-modulated onto the carrier using binary phase-shift keying with suppressed carrier using rectangular pulses.<sup>9</sup> The receiver, in turn, implements both carrier and symbol tracking, as well as demodulation and frame synchronization.

The prototype outputs several files after each simulation run:

- Uplink-transmitted symbols: This file contains a list of all symbols and their departure times in ground-station seconds. The file also includes a marker to indicate the start of each RCW. The meaning of *a symbol* depends on whether the uplink operates in the RF or optical domain.
- Uplink-received samples: This file contains a list of all samples arriving to the spacecraft, corrected for the one-way light-time delay and noise, and expressed in spacecraft seconds. The meaning of *a sample* depends on whether the uplink operates in the RF or optical domain.
- Downlink-transmitted symbols: This file contains a list of all PPM symbols to be sent in the downlink. The departure times may optionally be recorded as well in spacecraft seconds. This assumes that the downlink always operates in the optical domain.
- Downlink-received photons: This file contains a list of all photon arrivals at the ground station, in ground-station seconds. This assumes that the downlink always operates in the optical domain.

---

<sup>9</sup>Other formats could also be tested, but we selected this signaling for simplicity.

- Spacecraft measurements: Binary file containing the phase measurements collected during the simulation on board the spacecraft. These are encoded based on a newly proposed CCSDS standard for optical ranging, and can be used for interoperability testing purposes between multiple implementations.

Additionally, all information produced by the ground station is stored, including the recovered symbol and super-symbol clock, as well as the measured time of arrival of each RCW and its corresponding RCID.

#### A. Uplink and Downlink Channels

The prototype implements different uplink and downlink channels depending on whether the simulated link operates in the RF or optical domain. In all cases, however, two effects are modeled: Noise, which we assume Gaussian-distributed in the RF links and Poisson-distributed in the optical links; and the effect of the range-rate, which we model by assuming that during a ranging track the distance between the spacecraft and the Earth station can be approximated by a linear function of the form

$$\tau(t) = \tau_0 + \gamma t, \quad (2)$$

where  $\tau_0$  is the one-way propagation delay at the start of the ranging track,  $\gamma = \frac{r}{c}$ ,  $r$  is the range rate, and  $c$  is the speed of light. As noted in [1], assuming the same linear dynamics in both the uplink and downlink results in a two-way propagation delay equal to

$$\tau_{ud}(t) = \tau_u(t) + \tau_d(t + \tau_d(t)) = (2 + \gamma)(\tau_0 + \gamma t) \approx 2(\tau_0 + \gamma t). \quad (3)$$

Finally, because the HPE optical standard defines a non-coherent signaling format that is received via direct detection with a sufficiently wide bandpass filter, the optical channel need not model any Doppler effects on the received carrier. Alternatively, the RF signaling schemes used in space communications always rely on phase modulations, so phase rotations due to the range rate must be accounted for and corrected at the receiver. In that sense, it is well known that the non-relativistic Doppler shift induced by the relative motion between the spacecraft and the Earth station is approximately equal to

$$f_d(t) \approx -\frac{\dot{d}(t)}{\lambda}, \quad (4)$$

where  $d(t)$  is the distance over time, and  $\lambda$  is the carrier wavelength. Therefore, making the simplifying assumption that  $\tau(t) \propto d(t)$ , we get that  $f_d(t)$  will be constant over the ranging track.

## IV. Results

This section presents results obtained using the software prototype described in Section III. It is intended to showcase the feasibility of implementing the proposed

asynchronous ranging system under different uplink and downlink conditions, rather than providing comprehensive results on the achievable range error that could be recovered operationally. For example, all results presented show the estimated range error using single-shot estimates of the RTLT, as generated by the ranging system previously described. Additional range error reductions are possible with further post-processing, by averaging if the spacecraft dynamics are low, by performing linear regressions if the spacecraft is known to fly at constant velocity, etc. In other words, the results shown in the following subsections should not be considered the theoretical performance limit of an asynchronous ranging system.

#### **A. Scenario Description: The DSOC Terminal**

The results reported in this article are based on configuration parameters representative of the DSOC terminal that is scheduled to fly on board the Psyche spacecraft. In particular, estimates of range, range rate, signal and noise photon flux, and signal-to-noise conditions were obtained using spacecraft trajectory predicts together with basic information about DSOC and Psyche’s RF telecommunications subsystem (see Reference [1] for further details). For optical uplinks and downlinks, it was assumed that links were established from the Optical Communications Telescope Laboratory (OCTL) and the Palomar Observatory, respectively. RF links, in contrast, were established via a traditional Deep Space Network (DSN) 34-meter antenna. Finally, as a representative operational point in deep space, all simulations were conducted assuming Psyche was 1 astronomical unit (AU) away from Earth.

Next, we describe high-level configuration parameters for the different parts of the communication system. In particular, we assume that:

- The DSOC terminal is equipped with a 22-cm aperture and a 4-W transmit laser.
- The Psyche spacecraft is equipped with a 2-m high gain antenna connected to a radio with a noise factor of 3.2 dB. When pointing towards Earth, we assume that the antenna’s noise temperature is 25 K, i.e., the Psyche asteroid is not in the field of view.
- The Palomar Observatory has a 5-m aperture connected to an optical receiver. In turn, OCTL has a 1-m telescope connected to a system of lasers capable of providing 5 kW of optical power.
- The DSN 34-m antennas have a gain of approximately 66.75 dB and output an RF power of 20 kW.

#### **B. Test 1: Ranging with a PN Sequence and HPE Telemetry**

In this test, we assumed that the asynchronous ranging system was operated in a hybrid mode, with a PN sequence in the RF uplink, and HPE telemetry in the optical

downlink. Details on the signaling parameters for both links, as well as the assumed channel conditions, are reported in the tables of Figure 5. Importantly, we assumed that the spacecraft experiences a residual range rate of 10 m/s, equivalent to a Doppler shift in the uplink of 240 Hz, approximately. For reference, the DSN typically operates with residual Doppler shifts significantly smaller than this value during spacecraft cruise conditions, so this represents a moderate stress test for the ranging system.

Parameter	Uplink	Units
Frequency	7.2	GHz
PN code	T2B	-
Residual range rate	10	m/s
Chip rate	2.0686	Mcps
Chip SNR	12.3	dB

(a) Uplink Parameters

Parameter	Downlink	Units
Signal photons/slot	5.35	ph/slot
Noise photons/slot	0.16	ph/slot
Residual range rate	10	m/s
Slot width	16	ns
Modulation order	128	-
Repeat factor	1	Symbols
Code rate	1/3	-
Information rate	0.9	Mbps

(b) Downlink Parameters

Figure 5. Link configuration parameters for Test 1.

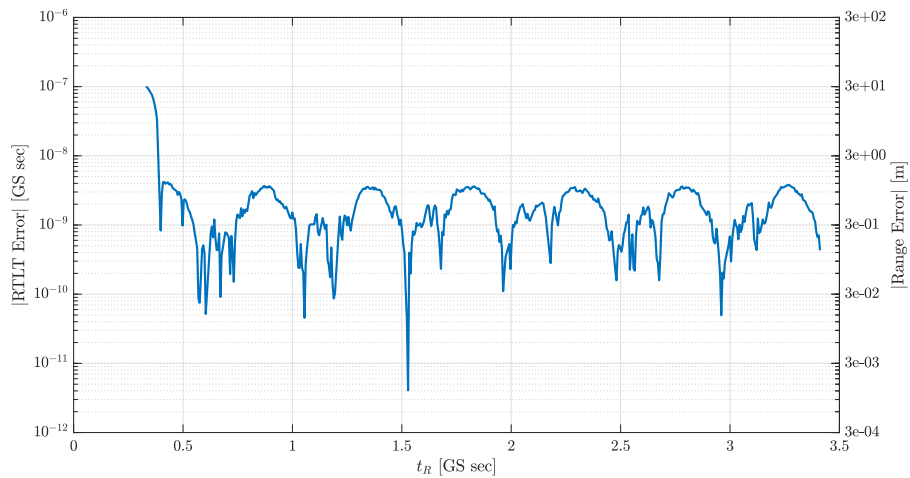


Figure 6. Round-Trip Light-Time and Range Error.

Figure 6 shows the RTLTL and range error obtained with the asynchronous ranging system. Results are reported in terms of the absolute value of the error as a function of ground station (GS) seconds and assuming that the conversion between RTLTL and range is constant and equal to  $c/2$ . Several remarks follow:

- Initially, the system does not output a range estimate. This represents the period of time where the spacecraft and ground station receivers are still not synchronized and, consequently, the range measurements are not valid.
- Removing any transient values, the range estimate has a bias of 25 cm and a standard deviation of 16 cm, approximately. As shown in [1], biases are

introduced by the synchronization mechanisms, but they can be systematically estimated and removed, a step not performed in this analysis for simplicity. The standard deviation, in turn, is driven by noise and imperfections in the implementation of the receiver algorithms.

- Even after reaching steady state operation, the range error exhibits a clear oscillatory pattern, ranging from less than 1 cm to 50 cm approximately. This source of error has been traced to the slot synchronization mechanism on the ground station receiver, which is based on the methods described in [11]. Further optimization of the receiver parameters (e.g., number of PPM symbols used, loop bandwidth) could be used to improve the range error estimate, a step not pursued because the obtained measurements are already below 1-meter accuracy.

### C. Test 2: RF Uplink with Data and HPE Telemetry

Next, we consider the case where the asynchronous ranging system is operated with an RF uplink carrying commanding information and an optical downlink using HPE telemetry. The configuration parameters for this test are provided in Figure 7 and assume that the uplink operates at a information rate of 175 kbps and that the symbol energy to noise spectral density is fairly high, at 12.3 dB. In the downlink direction, the conditions used during the first test are assumed here too.

			Parameter	Downlink	Units
			Signal photons/slot	5.35	ph/slot
			Noise photons/slot	0.16	ph/slot
			Residual range rate	10	m/s
			Slot width	16	ns
			Modulation order	128	-
			Repeat factor	1	Symbols
			Code rate	1/3	-
			Information rate	0.9	Mbps

Parameter	Uplink	Units
Frequency	7.2	GHz
Transfer frame length	1024	bits
Code	BCH (64,56)	-
Symbol rate	200	ksps
Symbol SNR	22.49	dB
Residual range rate	10	m/s

(a) Uplink Parameters
(b) Downlink Parameters

Figure 7. Link configuration parameters for Test 2.

Figure 8 presents the RTLT and ranging error values obtained from the test as a function of the ground station recording time. Once again, the limiting factor in the system is the performance of the slot synchronizer in the downlink due to the moderate signal and noise conditions in the downlink, which takes about 0.5 second to achieve lock and then produces periodic slips that generate outliers in the recovered range estimates. Post-processing the obtained data to remove these outliers results in a range bias estimate of 0.7 m and a 1-sigma uncertainty of 0.54 m.

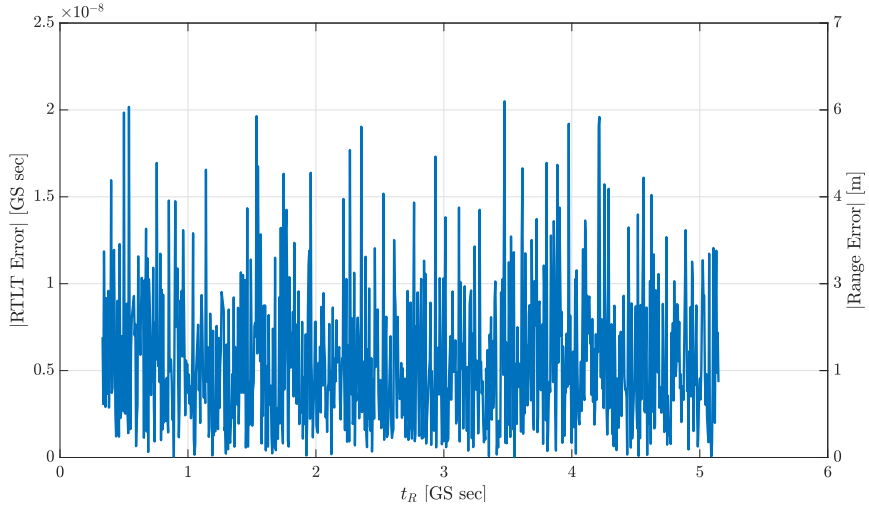


Figure 8. Round-Trip Light-Time and Range Error.

#### D. Test 3: HPE Telemetry on Uplink and Downlink

Finally, the last test performed assumes that both the uplink and downlink utilize HPE Telemetry. The exact link configuration are given in the tables of Figure 9 and have been derived from the link analysis inherited from Reference [1]. Also, to keep tests consistent, we have assumed that the downlink channel conditions and signal format are constant, as is the residual range rate (after post-compensation).

Parameter	Uplink	Units	Parameter	Downlink	Units
Signal photons/slot	6.86	ph/slot	Signal photons/slot	5.35	ph/slot
Noise photons/slot	0.47	ph/slot	Noise photons/slot	0.16	ph/slot
Residual range rate	10	m/s	Residual range rate	10	m/s
Slot width	512	ns	Slot width	16	ns
Modulation order	128	-	Modulation order	128	-
Repeat factor	1	Symbols	Repeat factor	1	Symbols
Code rate	1/3	-	Code rate	1/3	-
Information rate	0.028	Mbps	Information rate	0.9	Mbps

(a) Uplink Parameters

(b) Downlink Parameters

Figure 9. Link configuration parameters for Test 3.

The results for this test are reported in Figure 10. In this case, we observe that the system converges to a range bias of 3 meters, approximately, and a range uncertainty of 2.25 meters. As with previous results, most of this error is attributable to the noise conditions of both the uplink and downlink (although there is no phase measurement in the downlink, the ground station does need to record the time of arrival of each downlink RCW) and is driven mainly by the operation of the slot synchronizer. Furthermore, unlike previous tests, large synchronization slips can be observed in the simulation data, resulting in large spikes in Figure 10. Such large errors are typically

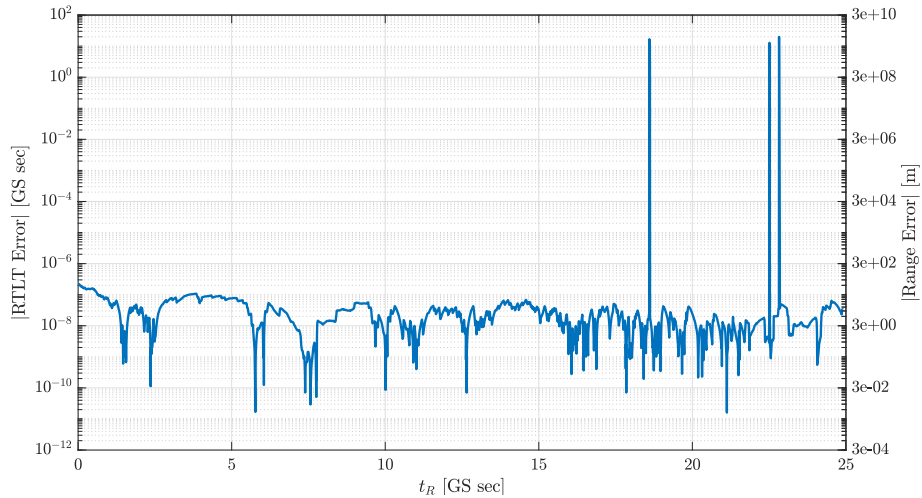


**Figure 10. Round-Trip Light-Time and Range Error.**

driven by errors while recording the RCID of either the uplink or downlink RCWs and can be eliminated either in operations by recovering the RCIDs from decoded data or in post-processing by removing data outliers that are beyond plausible range uncertainty bounds.

## V. Conclusions and Future Work

This article describes an asynchronous ranging system to recover range information between a spacecraft and a ground station on Earth. Measurements for the range computation are obtained on the ground station’s uplink subsystem, and on the spacecraft’s uplink receiver, thus eliminating the requirement to synchronize the uplink and downlink transmissions on board the spacecraft. Because most spacecraft do not have an accurate enough clock for time-tagging their phase measurements, the instant of time at which that value is recorded is triggered from the spacecraft downlink transmit subsystem, every time a downlink ranging frame departs. Then, on the ground station receiver, the reception of these frames is time-tagged, and the measurement recorded on board the spacecraft is associated with said time-tag recorded. Finally, to ensure that enough range ambiguity is available, the duration of the ranging codewords can be selected during mission design, and range codeword identifiers are used to differentiate between them.

This article also describes a software prototype developed at JPL to validate the concept and operation of the ranging system. The prototype currently accepts several uplink formats, including HPE telemetry, RF commanding data, and a PN ranging sequence (future enhancements will allow the use of HPE Beacon with accompanying data). In the downlink direction, only HPE telemetry is allowed, and both RTLT and range measurements are recovered from the available observables. To validate the system operation, the prototype also includes functions to calculate the theoretical



RTLT and range values given a linear spacecraft trajectory, thus allowing computation of range and RTLT error.

## Acknowledgments

I would like to acknowledge Jon Hamkins and Ryan Rogalin for their thorough review and significant contributions to this article. I would also like to acknowledge Abhijit Biswas and Meera Srinivasan for providing trajectory information for DSOC and Hua Xie for using her optical link budget tool to estimate the optical uplink and downlink performance.

The research was carried out at the Jet Propulsion Laboratory, California Institute of Technology, under a contract with the National Aeronautics and Space Administration (80NM0018D0004).

## References

- [1] M. Sanchez Net, “Optical Ranging: Synchronous-Mode Concept, Prototype, and Validation,” *The Interplanetary Network Progress Report*, vol. 42-229, Jet Propulsion Laboratory, Pasadena, California, pp. 1–47, May 15 2022.  
[https://ipnpr.jpl.nasa.gov/progress\\_report/42-229/42-229B.pdf](https://ipnpr.jpl.nasa.gov/progress_report/42-229/42-229B.pdf)
- [2] M. Sanchez Net and J. Hamkins, “Optical Telemetry Ranging,” *The Interplanetary Network Progress Report*, vol. 42-221, Jet Propulsion Laboratory, Pasadena, California, pp. 1–23, May 15 2020. [https://ipnpr.jpl.nasa.gov/progress\\_report/42-221/42-221B.pdf](https://ipnpr.jpl.nasa.gov/progress_report/42-221/42-221B.pdf)
- [3] J. Hamkins, P. Kinman, H. Xie, V. Vilnrotter, and S. Dolinar, “Telemetry Ranging: Concepts,” *The Interplanetary Network Progress Report*, vol. 42-203, Jet Propulsion Laboratory, Pasadena, California, pp. 1–20, November 15 2015.  
[https://ipnpr.jpl.nasa.gov/progress\\_report/42-203/203C.pdf](https://ipnpr.jpl.nasa.gov/progress_report/42-203/203C.pdf)
- [4] J. Hamkins, P. Kinman, H. Xie, V. Vilnrotter, S. Dolinar, N. Adams, E. Sanchez, and W. Millard, “Telemetry Ranging: Laboratory Validation Tests and End-to-End Performance,” *The Interplanetary Network Progress Report*, vol. 42-206, Jet Propulsion Laboratory, Pasadena, California, pp. 1–35, August 15 2016.  
[https://ipnpr.jpl.nasa.gov/progress\\_report/42-206/206D.pdf](https://ipnpr.jpl.nasa.gov/progress_report/42-206/206D.pdf)
- [5] Consultative Committee for Space Data Systems, “Optical Communications Physical Layer,” Tech. Rep. CCSDS 141.0-B-1, August 2019.  
<https://public.ccsds.org/Pubs/141x0b1.pdf>
- [6] —, “Optical Communications Coding and Synchronization,” Tech. Rep. CCSDS 142.0-B-1, August 2019. <https://public.ccsds.org/Pubs/142x0b1.pdf>
- [7] —, “TC Synchronization and Channel Coding,” Tech. Rep. CCSDS 231.0-B-4, July 2021. <https://public.ccsds.org/Pubs/231x0b4e0.pdf>
- [8] —, “TM Synchronization and Channel Coding,” Tech. Rep. CCSDS 131.0-B-4, April 2022. <https://public.ccsds.org/Pubs/131x0b4.pdf>
- [9] —, “Radio Frequency and Modulation Systems—Part 1: Earth Stations and Spacecraft,” Tech. Rep. CCSDS 401.0-B-32, October 2021.  
<https://public.ccsds.org/Pubs/401x0b32.pdf>

- [10] —, “Pseudo-Noise (PN) Ranging Systems,” Tech. Rep. CCSDS 414.1-B-3, January 2022. <https://public.ccsds.org/Pubs/414x1b3.pdf>
- [11] R. Rogalin and M. Srinivasan, “Synchronization for Optical PPM with Inter-Symbol Guard Times,” *The Interplanetary Network Progress Report*, vol. 42-209, Jet Propulsion Laboratory, Pasadena, California, pp. 1–19, May 15 2017. [https://ipnpr.jpl.nasa.gov/progress\\_report/42-209/209C.pdf](https://ipnpr.jpl.nasa.gov/progress_report/42-209/209C.pdf)